Modeling and Analysis of Mixed Traffic Networks with Human-driven and Autonomous Vehicles

Qing Xu
Tsinghua University

Chaoyi Chen (chency19@mails.tsinghua.edu.cn)
Tsinghua University https://orcid.org/0000-0002-2158-7969

Xueyang Chang
Tsingcloud Co. Lmt.

Dongpu Cao
University of Waterloo

Mengchi Cai
Tsinghua University

Jiawei Wang
Tsinghua University

Keqiang Li
Tsinghua University

Jianqiang Wang
Tsinghua University

Original Article

Keywords: Macroscopic traffic model, Connected and automated vehicle, Traffic Coordination

Posted Date: November 15th, 2021

DOI: https://doi.org/10.21203/rs.3.rs-1053566/v1

Modeling and Analysis of Mixed Traffic Networks with Human-driven and Autonomous Vehicles

Qing Xu[1], Chaoyi Chen[1,*], Xueyang Chang[2], Dongpu Cao[3],
Mengchi Cai[1], Jiawei Wang[1], Keqiang Li[1] and Jianqiang Wang[1].

***Abstract*—The emergence of connected and automated vehicles (CAV) indicates improved traffic mobility in future traffic transportation systems. This study addresses the research gap in macroscopic traffic modeling of mixed traffic networks where CAV and human-driven vehicles coexist. CAV behavior is explicitly included in the proposed traffic network model, and the vehicle number non-conservation problem is overcome by describing the approaching and departure vehicle number in discrete time. The proposed model is verified in typical CAV cooperation scenarios. The performance of CAV coordination is analyzed in road, intersection and network scenario. Total travel time of the vehicles in the network is proved to be reduced when coordination are applied. Simulation results validate the accuracy of the proposed model and the effectiveness of the proposed algorithm.**

***Index Terms*—Macroscopic traffic model, Connected and automated vehicle, Traffic Coordination.**

I. Introduction

CONNECTED and automated vehicles (CAV) are a promising technology to solve traffic accidents and congestion problems in urban traffic networks, and it has widely attracted the attention of academia and industries towards its research and development.

Despite the benefits brought by CAV to traffic mobility, their influence on the macroscopic traffic network model has rarely been studied. Traditional macroscopic traffic network modeling uses hydro-mechanics modeling to formulate the relationship between vehicle speed and car-following distance [1]. METANET is a widely-used highway traffic network simulation platform, employing a steady-state second-order equation to model the flow distribution and traffic state parameters [2]–[4]. Inspired by Lighthill-Whitham-Richards traffic flow model [5], [6], some multi-lane models based on the Aw-Rascle methods have also been proposed [7]–[9]. In urban traffic network modeling, intersections are inevitable traffic nodes with traffic lights. [10], [11] used cellular automata to model traffic flows at urban nonsignalized intersections. [12], [13] established the equilibrium equation for roads and distribution equation for intersections. Petri net [14], [15], fundamental diagram [16], [17] and Berg-Lin-Xi (BLX) model [18], [19] have also been used to model the intersection traffic network.

When CAVs are involved, most research focuses on fully-autonomous scenarios [20]. Research on single CAV coordination can be classified into several categories. For longitudinal control in straight roads, several multi-vehicle coordination methods have been proposed, *e.g.*, vehicle platoon control [21], cooperative adaptive cruise control (CACC) [22], and cooperative collision avoidance [23]. In intersection scenarios, coordinated control through V2I and V2V technologies has been widely discussed, *e.g.*, cooperative on-ramp merging [24], hierarchical optimization [25], and CAV scheduling [26]. As for cooperation in lateral control, V2V communication improves CAV's lane change performance [27] and enables cooperative multi-vehicle lane change [28] or formation control [29]. Other research also focuses on the path planning [30] and vehicle joint control [31].

However, the current transportation system will take decades to transform fully into CAV systems. A more practical scenario in the near future is a mixed traffic environment where CAVs and human-driven vehicles (HDVs) coexist [32], [33]. [34] derived the fundamental flow and density diagram, assuming that CAVs have a shorter headway time. The delay time caused by vehicles' stop-and-go behavior is reduced in a mixed traffic environment. [35] pointed out that introducing CAVs into existing traffic environments may lower the traffic efficiency because of their conservative driving strategies. Similar results were observed in [36]. [37], [38] studied the impact of autonomous vehicles on traffic flow through theoretical traffic flow analysis, clarifying changes in the key traffic flow parameters with increasing market penetration rates (MPRs).

Traffic optimization methods for mixed traffic networks differ from that of traditional networks, although both influence traffic network modeling. Traffic signal and phasing time (SPAT) control is the most common method to optimize traffic networks. Based on the traffic network model of [13], [39] established a nonlinear optimization method for signal light control that minimizes the number of vehicles in a network. [40] further designed a linear quadratic optimal controller to increase the calculation efficiency. [41] used the BLX and S model (a simplified BLX model) to design the model predictive control (MPC) that minimizes the total travel time in the network. Minimizing the queuing length in the network is another common optimization goal, and several methods

This work was supported by the National Natural Science Foundation of China under Grant 52072212, China Intelligent and Connected Vehicles (Beijing) Research Institute Co., Ltd., Dongfeng Automobile Co., Ltd and Key-Area Research and Development Program of Guangdong Province under Grant 2019B090912001. *(*Corresponding author: Chaoyi Chen)*

[1]Qing Xu, Chaoyi Chen, Jianqiang Wang, and Keqiang Li are with the School of Vehicle and Mobility, Tsinghua University. (e-mail: {qingxu, likq, wjqlws}@tsinghua.edu.cn), ({chency19, cmc18, wangjw18}@mails.tsinghua.edu.cn).

[2]Xueyang Chang is with the Tsingcloud Co., Lmt. (e-mail: changxueyang11@163.com).

[3]D. Cao are with CogDrive lab, Department of Mechanical and Mechatronics Engineering, University of Waterloo, ON N2L 3G1, Canada. (e-mail: dp_cao2016@163.com).

have been applied to solve the problem, *e.g.*, greedy-based MPC [17] and PID controller [16]. [42], [43] proposed a hierarchical control method, which decoupled the network into several sub-networks. In the upper layer, MPC controls the in and out traffic flow of sub-networks to maximize the traffic throughput, while in the lower layer, MPC controls the traffic SPAT in each sub-network based on the S model to minimize the travel time. Analogously, [44] modified the upper layer control optimization objective under the same hierarchical framework.

Coordinated route allocation is another effective way to balance the traffic load in a network. [45] used mixed integer programming to solve the dynamic vehicle allocation problem. [46], [47] tested a distributed controller for CAVs and simulated different traffic loads, MPRs, and communication ranges. In addition, rule-based [48] and greedy-based searching algorithms [49] were also used in previous research. [50] used theoretical traffic analysis and found inappropriate traffic allocation to increase the total delay time in the network as MPR increases. [51] proposed a CAV path guidance method in a mixed traffic network. The path planning of CAV and HDV are considered using a graph-based traffic network model. By establishing the corresponding nonlinear programming problem, CAV coordination route planning was found to increase traffic efficiency.

Because existing macroscopic traffic models are insufficient for mixed traffic environments, we propose a macroscopic traffic model for mixed traffic networks to address the lack of research on coordinated CAV route allocation in an urban traffic network. Then, we design typical algorithms in CAV coordination scenarios to verify the effectiveness of the proposed model. A network-based route allocation algorithm is further established to increase traffic efficiency. Specifically, our contributions are as follows:

(1) A macroscopic model of a mixed traffic network is proposed, with MPRs and traffic flow characteristics as model descriptions. The existing BLX model [18] may lead to vehicle number non-conservation problem, which is solved by explicitly including the CAVs as parameter in modeling.
(2) Several coordination algorithms are verified on the proposed model, including CAV coordination on straight roads, intersections, and route allocation. A network-based optimization algorithm is proposed to minimize the total travel time of vehicles in the network.
(3) The effectiveness of the proposed macroscopic mixed traffic model is validated with a feasible precision. The proposed coordination algorithm is shown to increase traffic efficiency in various MPRs.

The rest of this paper is organized as follows. Section II introduces the proposed mixed traffic network modeling method. Section III presents the three coordination methods applied to the proposed model. The simulation results are shown in Section IV. Finally, Section V concludes this paper.

II. Modeling of Mixed Traffic in Urban Road Network

This paper proposes an urban road network traffic model based on the S model in [41] for mixed traffic flow control in different MPRs.

A. Approaching traffic network modeling

The network traffic model is described in discrete time with sampling period T_{s} and time instant k. Each road is divided into two sections: free-driving and queuing zones. The vehicles entering road (u,d) firstly drive through the free-driving zone and then get stuck in the queuing zone. Because the queuing zone dynamically changes with time k, the average length of the free-driving zone $L_{u,d}^{\mathrm{mov}}(k)$ is calculated as

$$L_{u,d}^{\mathrm{mov}}(k) = L_{u,d} - \frac{q_{u,d}(k)\cdot l_{\mathrm{veh}}^{\mathrm{que}}}{N_{u,d}^{\mathrm{lane}}}, \tag{1}$$

where, $L_{u,d}$ is the length of the road, $q_{u,d}(k)$ is the total number of vehicles in the queuing zone, $l_{\mathrm{veh}}^{\mathrm{que}}$ is the road length that one vehicle occupies in the queue, and $N_{u,d}^{\mathrm{lane}}$ is the lane number.

Denoting the average speed of the vehicles in free-driving zone $L_{u,d}^{\mathrm{mov}}(k)$ as $v_{u,d}(k)$, the vehicle travel time through the free-driving zone is defined as $\tau_{u,d}(k)$. Because we use the discrete time modeling method, the travel time is divided into integer part $\delta_{u,d}(k)$ and fractional part $\gamma_{u,d}(k)$ as

$$\tau_{u,d}(k) = \delta_{u,d}(k) + \gamma_{u,d}(k), \tag{2}$$

$$\delta_{u,d}(k) = \mathrm{floor}(\tau_{u,d}(k)), 0 \le \gamma_{u,d}(k) < 1. \tag{3}$$

It can be calculated by solving

$$\begin{aligned} L_{u,d}^{\mathrm{mov}}(k) =& T_{\mathrm{s}} \sum_{i=1}^{\delta_{u,d}(k)} v_{u,d}(k-i) + \\ & T_{\mathrm{s}}\cdot\gamma_{u,d}(k)\cdot v_{u,d}(k-\delta_{u,d}(k)-1), \end{aligned} \tag{4}$$

where $v_{u,d}(\cdot)$ is the average moving vehicle speed on the free-driving zone. Assuming that the moving traffic flow is continuous, $v_{u,d}(\cdot)$ is calculated using the macroscopic traffic flow model with traffic flow density $K_{u,d}(k)$ defined as

$$K_{u,d}(k) = \frac{n_{u,d}(k) - q_{u,d}(k)}{N_{u,d}^{\mathrm{lane}}\cdot L_{u,d}^{\mathrm{mov}}(k)}, \tag{5}$$

where $n_{u,d}(k)$ is the total number of vehicles on road (u,d) at time k.

The macroscopic traffic flow model in [52] is adopted to describe the relationship between the average vehicle speed and traffic flow density.

$$v_{u,d}(k) = \begin{cases} v^{\mathrm{free}}, & \text{if } K_{u,d}(k) \le K^{\mathrm{free}}, \\ v_{\mathrm{ncop}}(K_{u,d}(k)), & \text{if } K^{\mathrm{jam}} < K_{u,d}(k) < K^{\mathrm{free}}, \\ v^{\mathrm{jam}}, & \text{if } K_{u,d}(k) \ge K^{\mathrm{jam}}, \end{cases} \tag{6}$$

$$v_{\mathrm{ncop}}(K_{u,d}(k)) = v^{\mathrm{jam}} + (v^{\mathrm{free}} - v^{\mathrm{jam}})\cdot K_{\mathrm{adj}}^{b}, \tag{7}$$

$$K_{\mathrm{adj}} = 1 - \left(\frac{K_{u,d}(k) - K^{\mathrm{free}}}{K^{\mathrm{jam}} - K^{\mathrm{free}}}\right)^{a}, \tag{8}$$

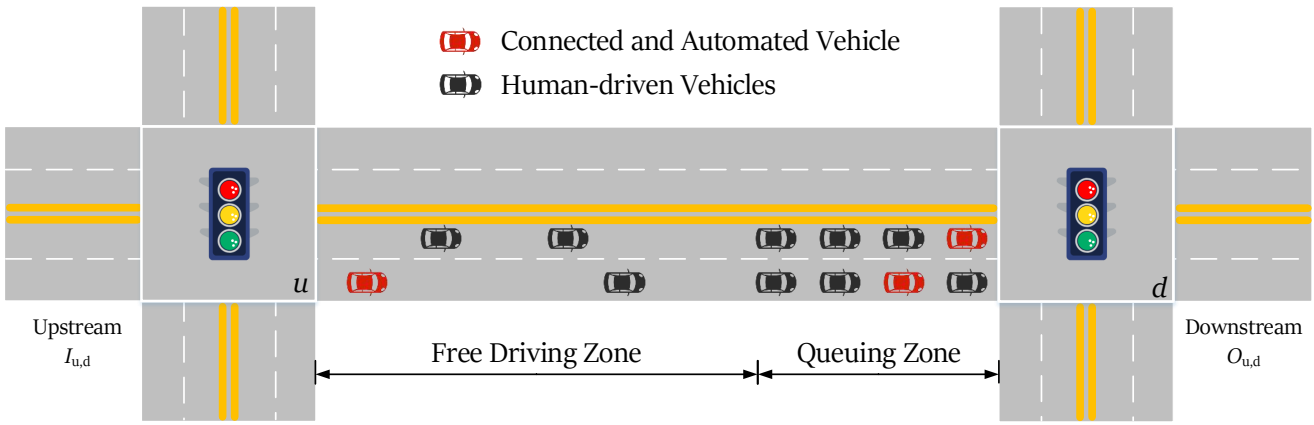

Fig. 1: Illustration of road segmentation. Road (u, d) is separated into two sections: free driving zone where vehicles move with the traffic flow and queuing zone where they are idling due to traffic lights. Both connected and automated vehicles and human-driven vehicles are considered in the modeling. The upstream and downstream sets are denoted as $I_{\mathrm{u,d}}$ and $O_{\mathrm{u,d}}$, respectively.

where $K^{\mathrm{free}} = 1/l_{veh}^{\mathrm{free}}$ and $K^{\mathrm{jam}} = 1/l_{veh}^{\mathrm{que}}$. v^{free} is the free-driving speed, which is the maximum on-road speed limit. v^{jam} is the vehicle speed in traffic jam. l_{veh}^{free} is the smallest road length occupation in free driving zone, which equals the vehicle length plus the minimum car following distance. Other parameters are chosen as $a = 2, b = 4$ in this study.

(1) shows that $\tau_{u,d}(k)$ is determined mainly by changes in $q_{u,d}(k)$, rendering it difficult to achieve the conservation of number of vehicles in the free-driving zone.

The instant of time when the last vehicle in the queuing zone leaves the upstream road is denoted as $k-1$, which is $\bar{\tau}_{u,d}$ period ahead of the current time and defined as

$$\bar{\tau}_{u,d} = \max(\tau_{u,d}(k-1), \tau_{u,d}(k), 1), \tag{9}$$

$$\bar{\tau}_{u,d}(k) = \bar{\delta}_{u,d}(k) + \bar{\gamma}_{u,d}(k), \tag{10}$$

$$\bar{\delta}_{u,d}(k) = \mathrm{floor}(\bar{\tau}_{u,d}(k)), 0 \leq \bar{\gamma}_{u,d}(k) < 1. \tag{11}$$

Then, the number of vehicles arriving at the queuing zone during time $[kT_{\mathrm{s}}, (k+1)T_{\mathrm{s}})$ is denoted as $m_{u,d}^{\mathrm{arr}}(k)$, which is calculated by

$$\begin{aligned}
&m_{u,d}^{\mathrm{arr}}(k) = \\
&\sum_{i \in I_{u,d}} \min\left(m_{i,u,d}^{\mathrm{dep,mov}}(k_{i,u,d}^{\mathrm{a}}), (1-\gamma_{u,d}(k)) \cdot m_{i,u,d}^{\mathrm{dep}}(k_{i,u,d}^{\mathrm{a}})\right) \\
&+ \sum_{i \in I_{u,d}} \min\left(m_{i,u,d}^{\mathrm{dep,mov}}(k_{i,u,d}^{\mathrm{b}}), \bar{\gamma}_{u,d}(k) \cdot m_{i,u,d}^{\mathrm{dep}}(k_{i,u,d}^{\mathrm{b}})\right) \\
&+ \sum_{t=\delta_{u,d}(k)-1}^{\bar{\delta}_{u,d}(k)} \sum_{i \in I_{u,d}} m_{i,u,d}^{\mathrm{dep,mov}}(k_{i,u,d}^{\mathrm{c}}), \\
&k_{i,u,d}^{\mathrm{a}} = k - \delta_{u,d}(k) - \sigma_{i,u,d}, \\
&k_{i,u,d}^{\mathrm{b}} = k - \bar{\delta}_{u,d}(k) - 1 - \sigma_{i,u,d}, \\
&k_{i,u,d}^{\mathrm{c}} = k - t - \sigma_{i,u,d},
\end{aligned} \tag{12}$$

where $I_{u,d}$ is the union set of all the upstream intersections of road (u, d) and $\sigma_{i,u,d}$ is the time spent driving through intersection u along route (i, u, d). $m_{i,u,d}^{\mathrm{dep}}(k)$ is the number of vehicles driving on road (u, d) from upstream road (i, u) at time k, and $m_{i,u,d}^{\mathrm{dep,mov}}(k)$ is the number of vehicles driving on the free-driving zone (u, d) from upstream road (i, u) at time k. $m_{i,u,d}^{\mathrm{dep,mov}}(k)$ is updated by

$$\begin{aligned}
&m_{i,u,d}^{\mathrm{dep,mov}}(k_{i,u,d}^{\mathrm{a}}) = \max\Big(m_{i,u,d}^{\mathrm{dep,mov}}(k_{i,u,d}^{\mathrm{a}}) \\
&-(1-\gamma_{u,d}(k)) \cdot m_{i,u,d}^{\mathrm{dep}}(k_{i,u,d}^{\mathrm{a}}), 0\Big), i \in I_{u,d},
\end{aligned} \tag{13}$$

$$\begin{aligned}
&m_{i,u,d}^{\mathrm{dep,mov}}(k_{i,u,d}^{\mathrm{b}}) = \max\Big(m_{i,u,d}^{\mathrm{dep,mov}}(k_{i,u,d}^{\mathrm{b}}) \\
&-\bar{\gamma}_{u,d}(k) \cdot m_{i,u,d}^{\mathrm{dep}}(k_{i,u,d}^{\mathrm{b}}), 0\Big), i \in I_{u,d},
\end{aligned} \tag{14}$$

$$\begin{aligned}
&m_{i,u,d}^{\mathrm{dep,mov}}(k - t - \sigma_{i,u,d}) = 0, i \in I_{u,d} \\
&t = \delta_{u,d}(k) - 1, \cdots, \bar{\delta}_{u,d}(k).
\end{aligned} \tag{15}$$

Remark 1: In the proposed traffic network model, the number of vehicles in the free-driving zone $m_{i,u,d}^{\mathrm{dep,mov}}(k)$ is used to update the incoming number of vehicles to the queuing zone $m_{u,d}^{\mathrm{arr}}(k)$, because the sole use of $\tau_{u,d}(k)$ to calculate the vehicle's entering time cannot guarantee the conservation of the number of vehicles. Vehicle travel time $\tau_{u,d}(k)$ is related to time-variant variables, namely, vehicle travel speed $v_{u,d}(k)$ and free-driving zone length $L_{u,d}^{\mathrm{mov}}(k)$. $v_{u,d}(k)$ is influenced by traffic flow state and multi-vehicle cooperation method, and $L_{u,d}^{\mathrm{mov}}(k)$ is related to queuing length $q_{u,d}(k)$.

B. Departure traffic network modeling

When vehicles enter a road, they change lanes to follow their desired routes. If no control on route selection is imposed, the number of vehicles selecting each route is given as

$$m_{u,d,o}^{\mathrm{arr}}(k) = \beta_{u,d,o}(k) \cdot m_{u,d}^{\mathrm{arr}}(k) \tag{16}$$

$$\sum_{o \in O_{u,d}} \beta_{u,d,o}(k) = 1 \tag{17}$$

where $O_{u,d}$ is the union set of the downstream intersections of road (u,d), and $\beta_{u,d,o}(k)$ is the route selection ratio.

The number of departing vehicles $m^{\text{dep}}_{u,d,o}(k)$ is related to three parameters: incoming number of vehicles from road (u,d), traffic load on the departure road (d,o) and traffic SPAT on route (u,d,o).

The number of vehicles on road (u,d) along route (u,d,o) during the period $[kT_{\text{s}},(k+1)T_{\text{s}})$ is then calculated as follows. Based on traffic light conditions, ($b_{u,d,o}(k)=1$ indicates green light), the maximum number of vehicles that depart the road (u,d) along route (u,d,o) is

$$\bar{m}^{\text{dep}}_{u,d,o}(k)=\begin{cases}\min\left(q_{u,d,o}(k)+m^{\text{arr}}_{u,d,o}(k),\right. & \text{if} b_{u,d,o}(k)=1,\\ \qquad\qquad \left. Q_{u,d,o}(k)\cdot T_s\right) & \\ 0, & \text{if} b_{u,d,o}(k)=0,\end{cases} \tag{18}$$

where $q_{u,d,o}(k)$ is the route queue number of vehicles and $Q_{u,d,o}(k)$ is the saturation traffic flow density. It is worth noting that traffic lights block the traffic flow and decide the vehicles' stop-and-go behavior. Because the vehicles need to re-accelerate to the original driving speed from their idling state, the traffic flow density gradually grows to saturation value $Q_{u,d,o}(k)$ and is modeled as follows:

$$Q_{u,d,o}(k)=\begin{cases}\min\left(Q_{u,d,o}(k-1)+dQ_0,\right. & \\ \left. Q^{\max}_{u,d,o}\right), & \text{if} b_{u,d,o}(k)=1,\\ 0, & \text{if} b_{u,d,o}(k)=0.\end{cases} \tag{19}$$

where dQ_0 is the traffic flow density increment in the vehicle acceleration process, and $Q^{\max}_{u,d,o}$ is the saturation maximum traffic flow density.

For downstream road (d,o), the total number of vehicles departing from upstream roads is

$$\bar{m}^{\text{dep,sum}}_{d,o}(k)=\sum_{i\in I_{d,o}}\bar{m}^{\text{dep}}_{i,d,o}(k). \tag{20}$$

We assume that the total number of vehicles entering road (d,o) will not exceed the available capacity of the road. The available capacity for each upstream route can be determined using

$$S_{u,d,o}(k)=\begin{cases}\frac{\bar{m}^{\text{dep}}_{u,d,o}(k)}{\bar{m}^{\text{dep,sum}}_{d,o}(k)}\cdot S^{\text{exp}}_{d,o}(k), & \text{if} \bar{m}^{\text{dep,sum}}_{d,o}(k)>0,\\ 0, & \text{if} \bar{m}^{\text{dep,sum}}_{d,o}(k)=0,\end{cases} \tag{21}$$

where $S_{u,d,o}(k)$ is the available capacity allocated by downstream (d,o) to road (u,d) , and $S^{\text{exp}}_{d,o}(k)$ is the expected available capacity that considers future occupancy of the current vehicles. The actual number of vehicles then departing road (u,d) along route (u,d,o) is

$$m^{\text{dep}}_{u,d,o}(k)=\min\left(\bar{m}^{\text{dep}}_{u,d,o}(k),S_{u,d,o}(k)\right), \tag{22}$$

$$m^{\text{dep,mov}}_{u,d,o}(k)=m^{\text{dep}}_{u,d,o}(k). \tag{23}$$

The queuing length of a route is calculated as

$$q_{u,d,o}(k+1)=q_{u,d,o}(k)+m^{\text{arr}}_{u,d,o}(k)-m^{\text{dep}}_{u,d,o}(k), \tag{24}$$

and that of a road as

$$q_{u,d}(k+1)=\sum_{o\in O_{u,d}}q_{u,d,o}(k+1). \tag{25}$$

The available capacity of road (u,d) in next time step $k+1$ considering the travel time through the intersection is

$$\begin{aligned}S_{u,d}(k+1)=&S_{u,d}(k)-\sum_{i\in I_{u,d}}m^{\text{dep}}_{i,u,d}(k-\sigma_{i,u,d})\\ &+\sum_{o\in O_{u,d}}m^{\text{dep}}_{u,d,o}(k).\end{aligned} \tag{26}$$

In this time step $k+1$, vehicles in the intersection approaching road (u,k) also influence the available road capacity.

$$\begin{aligned}S^{\text{exp}}_{u,d}(k+1)=&S^{\text{exp}}_{u,d}(k)-\sum_{i\in I_{u,d}}m^{\text{dep}}_{i,u,d}(k)\\ &+\sum_{o\in O_{u,d}}m^{\text{dep}}_{u,d,o}(k).\end{aligned} \tag{27}$$

The road capacity should not exceed the overall queuing vehicle amount, therefore

$$S_{u,d}(k)\le C_{u,d}=\frac{L_{u,d}\cdot N^{\text{lane}}_{u,d}}{l^{\text{que}}_{\text{veh}}}. \tag{28}$$

Hence, at next time step $k+1$, the number of vehicles not queuing on road (u,d) is

$$\begin{aligned}n^{\text{mov}}_{u,d}(k+1)=&n^{\text{mov}}_{u,d}(k)-m^{\text{arr}}_{u,d}(k)\\ &+\sum_{i\in I_{u,d}}m^{\text{dep}}_{i,u,d}(k-\sigma_{i,u,d}).\end{aligned} \tag{29}$$

Therefore, the total number of vehicles at next time step $k+1$ on road (u,d) is

$$n^{\text{tot}}_{u,d}(k+1)=n^{\text{mov}}_{u,d}(k+1)+q_{u,d}(k+1) \tag{30}$$

C. Mixed traffic network modeling

Based on the proposed model, MPRs in different traffic flows are further calculated. Analogous to the idea in (12), the number of CAVs arriving at the end of the queuing zone at each road during the period $[kT_{\text{s}},(k+1)T_{\text{s}})$ is calculated as

$$\begin{aligned}m^{\text{arr,CAV}}_{u,d}(k)=&\sum_{i\in I_{u,d}}\alpha^{\text{dep}}_{i,u,d}(k^{\text{a}}_{i,u,d})\cdot\min\Big(m^{\text{dep,mov}}_{i,u,d}(k^{\text{a}}_{i,u,d}),\\ &(1-\gamma_{u,d}(k))\cdot m^{\text{dep}}_{i,u,d}(k^{\text{a}}_{i,u,d})\Big)+\sum_{i\in I_{u,d}}\alpha^{\text{dep}}_{i,u,d}(k^{\text{b}}_{i,u,d})\cdot\\ &\min\Big(m^{\text{dep,mov}}_{i,u,d}(k^{\text{b}}_{i,u,d}),\bar{\gamma}_{u,d}(k)\cdot m^{\text{dep}}_{i,u,d}(k^{\text{b}}_{i,u,d})\Big)\\ &+\sum_{t=\delta_{u,d}(k)-1}^{\bar{\delta}_{u,d}(k)}\sum_{i\in I_{u,d}}m^{\text{dep,mov}}_{i,u,d}(k^{\text{c}}_{i,u,d})\cdot\alpha^{\text{dep}}_{i,u,d}(k^{\text{c}}_{i,u,d})\end{aligned} \tag{31}$$

where, $\alpha^{\text{dep}}_{i,u,d}(k)$ is the MPR of CAVs driving on road (u,d) through route (i,u,d) in time step k. The MPR of the CAVs at the queuing tail is given by

$$\alpha^{\text{arr}}_{u,d}(k)=\frac{m^{\text{arr,CAV}}_{u,d}(k)}{m^{\text{arr}}_{u,d}(k)} \tag{32}$$

If CAVs choose routes similar to HDVs, the numbers of CAVs arriving at the queuing tail of road (u,d) and heading to intersection o is

$$m_{u,d,o}^{\mathrm{arr,CAV}}(k) = \beta_{u,d,o}(k) \cdot m_{u,d}^{\mathrm{arr,CAV}}(k) \tag{33}$$

$$\alpha_{u,d,o}^{\mathrm{arr}}(k) = \frac{m_{u,d,o}^{\mathrm{arr,CAV}}(k)}{m_{u,d,o}^{\mathrm{arr}}(k)} \tag{34}$$

where $\beta_{u,d,o}(k)$ is the corresponding MPR.

The number of CAVs departing from road (u,d) to route (u,d,o) and their MPRs are calculated using

$$\begin{aligned} m_{u,d,o}^{\mathrm{dep,CAV}}(k) &= \begin{cases} m_{u,d,o}^{\mathrm{dep,CAV},1}(k), & \text{if} m_{u,d,o}^{\mathrm{dep}}(k) \le q_{u,d,o}(k), \\ m_{u,d,o}^{\mathrm{dep,CAV},2}(k), & \text{if} m_{u,d,o}^{\mathrm{dep}}(k) > q_{u,d,o}(k), \end{cases} \\ m_{u,d,o}^{\mathrm{dep,CAV},1}(k) &= \alpha_{u,d,o}^{\mathrm{que}}(k) \cdot m_{u,d,o}^{\mathrm{dep}}(k), \\ m_{u,d,o}^{\mathrm{dep,CAV},2}(k) &= \alpha_{u,d,o}^{\mathrm{que}}(k) \cdot q_{u,d,o}(k) \\ &\quad + \alpha_{u,d,o}^{\mathrm{arr}}(k) \cdot \left(m_{u,d,o}^{\mathrm{dep}}(k) - q_{u,d,o}(k) \right), \end{aligned} \tag{35}$$

$$\alpha_{u,d}^{\mathrm{dep}}(k) = \frac{m_{u,d}^{\mathrm{dep,CAV}}(k)}{m_{u,d}^{\mathrm{dep}}(k)}, \tag{36}$$

where $\alpha_{u,d,o}^{\mathrm{que}}(k)$ is the MPR of the queue on route (u,d,o).

At next time step $k+1$, the number of queuing CAVs on road (u,d) and heading to route (u,d,o) and their MPRs are

$$\begin{aligned} q_{u,d,o}^{\mathrm{CAV}}(k+1) &= \alpha_{u,d,o}^{\mathrm{que}}(k) \cdot q_{u,d,o}(k) + m_{u,d,o}^{\mathrm{arr,CAV}}(k) \\ &\quad - m_{u,d,o}^{\mathrm{dep,CAV}}(k), \end{aligned} \tag{37}$$

$$\alpha_{u,d,o}^{\mathrm{que}}(k+1) = \frac{q_{u,d,o}^{\mathrm{CAV}}(k+1)}{q_{u,d,o}(k+1)}. \tag{38}$$

$$\tag{39}$$

The number of total queuing CAVs on road (u,d) at next time step $k+1$ is

$$q_{u,d}^{\mathrm{CAV}}(k+1) = \sum_{o \in O_{u,d}} q_{u,d,o}^{\mathrm{CAV}}(k). \tag{40}$$

$$\tag{41}$$

The number of free-driving CAVs on road (u,d) and their MPRs are

$$\begin{aligned} n_{u,d}^{\mathrm{mov,CAV}}(k+1) &= n_{u,d}^{\mathrm{mov,CAV}}(k) - m_{u,d}^{\mathrm{arr,CAV}}(k) \\ &\quad + \sum_{i \in I_{u,d}} m_{i,u,d}^{\mathrm{dep,CAV}}(k - \sigma_{i,u,d}), \end{aligned} \tag{42}$$

$$\alpha_{u,d}^{\mathrm{mov}}(k+1) = \frac{n_{u,d}^{\mathrm{mov,CAV}}(k+1)}{n_{u,d}^{\mathrm{mov}}(k+1)}. \tag{43}$$

$$\tag{44}$$

The MPR of CAVs on free-driving zones is one of the most important parameters influencing the performance of a multi-vehicle coordination algorithm. The number of CAVs on road (u,d) and their MPRs are

$$n_{u,d}^{\mathrm{CAV}}(k+1) = n_{u,d}^{\mathrm{mov,CAV}}(k+1) + q_{u,d}^{\mathrm{CAV}}(k+1), \tag{45}$$

$$\alpha_{u,d}(k+1) = \frac{n_{u,d}^{\mathrm{CAV}}(k+1)}{n_{u,d}(k+1).} \tag{46}$$

CAVs influence traffic flow differently compared to HDVs, which requires modification of the traffic flow model. The influences of car-following and lane-changing performances of CAVs with different penetration rates are considered as follows. The shorter car-following time headway of CAVs than HDVs contributes to the higher CAV penetration rate, leading to a higher traffic density at a certain average vehicle speed [37]. Previous research also found that the lane-changing decision difference between CAVs and HDVs may deteriorate traffic mobility when MPR is low [53]. Hence, we model the traffic flow density ratio of CAV and HDV, $\eta_{\mathrm{lc}}^{\mathrm{mix}}(\alpha_{u,d}^{\mathrm{mov}}(k))$. Considering parameters in the traffic flow models (6) and (7), the maximum traffic flow densities in free-driving and queuing zones are calculated as

$$\begin{aligned} K_{u,d}^{*}(k) &= \frac{\eta_{\mathrm{lc}}^{\mathrm{mix}}(\alpha_{u,d}^{\mathrm{mov}}(k))}{\alpha_1 + \alpha_2 + l_{\mathrm{veh}}}, \\ \alpha_1 &= \alpha_{u,d}^{\mathrm{mov}}(k) \cdot v^{*} \cdot T_{\mathrm{CAV}}^{*}, \\ \alpha_2 &= (1 - \alpha_{u,d}^{\mathrm{mov}}(k)) \cdot v^{*} \cdot T_{\mathrm{HDV}}^{*}, \\ * &= \mathrm{freeorjam}. \end{aligned} \tag{47}$$

where $T_{\mathrm{CAV}}^{\mathrm{free}}$ and T_{HDV}^{*} are the car-following time headway in free-driving zones, and $T_{\mathrm{CAV}}^{\mathrm{jam}}$ and T_{jam}^{*} are the car-following time headway in queuing zones of CAV and HDV, respectively.

Therefore, the mixed traffic network model is written as

$$\begin{aligned} & v_{u,d}^{\mathrm{mix}}(k) = \\ & \begin{cases} v^{\mathrm{free}}, & K_{u,d}(k) \le K_{u,d}^{\mathrm{free}}(k), \\ v_{\mathrm{mix}}\left(K_{u,d}(k)\right), & K_{u,d}^{\mathrm{free}}(k) < K_{u,d}(k) < K_{u,d}^{\mathrm{jam}}(k), \\ v^{\mathrm{jam}}, & K_{u,d}(k) \ge K_{u,d}^{\mathrm{jam}}(k), \end{cases} \\ & v_{\mathrm{mix}}\left(K_{u,d}(k)\right) = v^{\mathrm{jam}} + \left(v^{\mathrm{free}} - v^{\mathrm{jam}}\right) \\ & \cdot \left(1 - \left(\frac{K_{u,d}(k) - K_{u,d}^{\mathrm{free}}(k)}{K_{u,d}^{\mathrm{jam}}(\mathrm{k}) - K_{u,d}^{\mathrm{free}}(k)}\right)^{a}\right)^{b}. \end{aligned} \tag{48}$$

from which the intersection maximum saturation flow rate can be calculated as

$$Q_{u,d,o}^{\mathrm{mix}}(k) = N_{u,d,o}^{\mathrm{lane}} \cdot \max\left(K \cdot v_{\mathrm{mix}}(K)\right) \tag{49}$$

where $N_{u,d,o}^{\mathrm{lane}}$ is the lane number on road (u,d) of route (u,d,o). For $v_{\mathrm{mix}}(K)$ calculation, if queuing exists, i.e., $q_{u,d,o}(k) > 0$, queuing MPR $\alpha_{u,d,o}^{\mathrm{que}}(k)$ is used. Otherwise, arriving MPR $\alpha_{u,d,o}^{\mathrm{arr}}(k)$ is used.

The main contributions of the proposed traffic model lie in the following aspects:

(1) The MPRs of CAVs on roads and routes are described as state variables during modeling. Therefore, the influence of mixed traffic and cooperative driving in different MPRs can be analytically modeled.
(2) In the original model, the occupation length of each vehicle is assumed to be a constant. The proposed macroscopic traffic flow model describes the relationship between the mean speed and traffic flow density in different conditions to reduce modeling errors.
(3) The traffic state updating is modified recursively, solving the non-conservation problem in the original model as vehicles approach the tail of the queuing zone.

(4) The departure behavior of vehicles is modified. The number of departing vehicles in upstream routes is determined considering the future spare capacity in the downstream road. It guarantees that the number of arriving vehicles will not exceed road capacity, further reducing the modeling error.

III. Coordinated Control Methods of CAVs

After modeling the mixed traffic network, coordination methods are applied to CAVs to optimize the traffic flow. In this study, three coordination methods are considered.

A. Road coordination

Road coordination is one of the most common application scenarios of CAVs, *e.g.*, CACC, cooperative lane-changing, and multi-lane formation control. These coordination methods reduce disturbances of the driving behaviour of HDVs on traffic flow and increase traffic mobility. In the proposed model, macroscopic benefits of CAV coordination are simplified as shortening car-following time headway compared to HDVs. Because modeling the accurate distribution of CAVs in traffic flow is difficult, the following estimation method is used for approximation. We assume that coordination is activated when there exist at least three consecutive CAVs in one lane.

If cooperation probability exceeds a given threshold, the traffic flow performance is improved according to the average MPR of the moving CAVs to the total number of moving vehicles on-road. The cooperation probability of n vehicles and m CAVs can be calculated as

$$\begin{aligned} P_{\mathrm{CAV},\geq 3}(n,m) &= 1 - \frac{N_{\mathrm{CAV},1} + N_{\mathrm{CAV},2}}{A_n}, \\ N_{\mathrm{CAV},1} &= A_{n-m} \cdot A_{n-m+1}^{m}, \\ N_{\mathrm{CAV},1} &= A_m \cdot A_{n-m} \sum_{i=1}^{\lfloor m/2 \rfloor} C_{n-m+1}^{i} \cdot C_{n-m+1-i}^{m-2i}, \end{aligned} \tag{50}$$

where A and C represents the total permutations and combinations, respectively.

The maximum traffic flow density in free-driving zone considering CAV coordination is calculated as

$$\begin{aligned} K_{u,d,\mathrm{co}}^{\mathrm{free}}(k) =& \eta_{\mathrm{lc}}^{\mathrm{coop}} \left(\alpha_{u,d}^{\mathrm{mov}}(k)\right) \\ & \cdot \left(\left(\alpha_{u,d}^{\mathrm{mov}}(k) - \alpha_{u,d,\mathrm{co}}^{\mathrm{mov}}(k)\right) \cdot v^{\mathrm{free}} \cdot T_{\mathrm{CAV}}^{\mathrm{free}} \right. \\ & + \alpha_{u,d,\mathrm{co}}^{\mathrm{mov}}(k) \cdot v^{\mathrm{free}} \cdot T_{\mathrm{CAV,co}} + \left(1 - \alpha_{u,d}^{\mathrm{mov}}(k)\right) \\ & \left. \cdot v^{\mathrm{free}} \cdot T_{\mathrm{HDV}}^{\mathrm{free}} + l_{\mathrm{veh}}\right)^{-1}, \\ \alpha_{u,d,\mathrm{co}}^{\mathrm{mov}}(k) =& f_{\mathrm{CAV,co}} \left(K_{u,d}(k) \cdot L_{u,d}^{\mathrm{mov}}(k), \alpha_{u,d}^{\mathrm{mov}}(k)\right), \end{aligned} \tag{51}$$

where $\eta_{\mathrm{lc}}^{\mathrm{coop}}$ is the mixed traffic flow density in CAV coordination, $\alpha_{u,d}^{\mathrm{mov}}(k)$ is the MPR of CAVs in mixed traffic, $f_{\mathrm{CAV,co}}$ is the function to calculate the average MPR from the number of vehicles, and $T_{\mathrm{CAV,co}}$ is the CAV headway distance. The road coordination method applied to CAV in the mixed traffic model is as follows:

$$\begin{aligned} & v_{u,d}^{\mathrm{coop}}(k) = \\ & \begin{cases} v^{\mathrm{free}}, & K_{u,d}(k) \leq K_{u,d,co}^{\mathrm{free}}(k), \\ v_{\mathrm{coop}}\left(K_{u,d}(k)\right), & K_{u,d,co}^{\mathrm{free}}(k) < K_{u,d}(k) < K_{u,d}^{\mathrm{jam}}(\mathrm{k}), \\ v^{\mathrm{jam}}, & K_{u,d}(k) \geq K_{u,d}^{\mathrm{jam}}(\mathrm{k}), \end{cases} \\ & v_{\mathrm{coop}}\left(K_{u,d}(k)\right) = v^{\mathrm{jam}} + \left(v^{\mathrm{free}} - v^{\mathrm{jam}}\right) \\ & \cdot \left(1 - \left(\frac{K_{u,d}(k) - K_{u,d,\mathrm{co}}^{\mathrm{free}}(k)}{K_{u,d}^{\mathrm{jam}}(\mathrm{k}) - K_{u,d,\mathrm{co}}^{\mathrm{free}}(k)}\right)^{a}\right)^{b}. \end{aligned} \tag{52}$$

TABLE I: Traffic parameters in road coordination.

Parameters	Values	Parameters	Values
T_{HDV}^{free}	1.5 s	T_{HDV}^{jam}	0.6 s
T_{CAV}^{free}	0.8 s	T_{CAV}^{jam}	0.3 s
$T_{\mathrm{CAV,co}}$	0.3 s	l_{veh}	7 m
v^{free}	road speed limit	v^{jam}	8 km/h

TABLE II: Traffic input parameters.

Index	Road (1,4) & (3,4)		Road (2,5) & (7,8)	
	Flow (veh/hr)	MPR (%)	Flow (veh/hr)	MPR (%)
1	720	20	432	12
2	1440	40	864	24
3	2160	60	1296	36
4	2880	80	1728	48
5	3600	100	2160	60

B. Intersection coordination

All CAVs in the same platoon can respond instantaneously to the traffic light turning green, leading to a higher flow rate with respect to penetration rate compared to pure HDV traffic. The improvements in $Q_{u,d,o}^{\mathrm{coop}}(k)$ are represented as a linear function of the CAV penetration rate in the queue of a route with corresponding increments of dQ^{coop}. The maximum saturation traffic flow density is calculated using

$$Q_{u,d,o}^{\mathrm{coop}}(k) = N_{u,d,o}^{\mathrm{lane}} \cdot \max(k \cdot v_{\mathrm{coop}}(k)). \tag{53}$$

To calculate the MPR and $v_{\mathrm{coop}}(k)$, when there is queuing on road, the queuing number of vehicles $q_{u,d,o}(k)$ and the MPR $\alpha_{u,d,o}^{\mathrm{que}}(k)$ are used. Otherwise, the arriving number of vehicles $m_{u,d,o}^{\mathrm{arr}}(k)$ and the MPR $\alpha_{u,d,o}^{\mathrm{arr}}(k)$ are used.

C. Network coordination

Routes of CAVs can be guided to balance traffic loads in the road network to mitigate traffic congestion caused by high traffic load. However, efficient microscopic routing of each CAV in the network is challenging for global load balance. Based on the proposed model, a macroscopic global routing method is adopted. The CAV route selection ratio, i.e., $\beta_{u,d,o}^{\mathrm{CAV,ctrl}}(k)$, is used as the control variable. To reduce the possibility that a CAV is unable to reach its destination due to

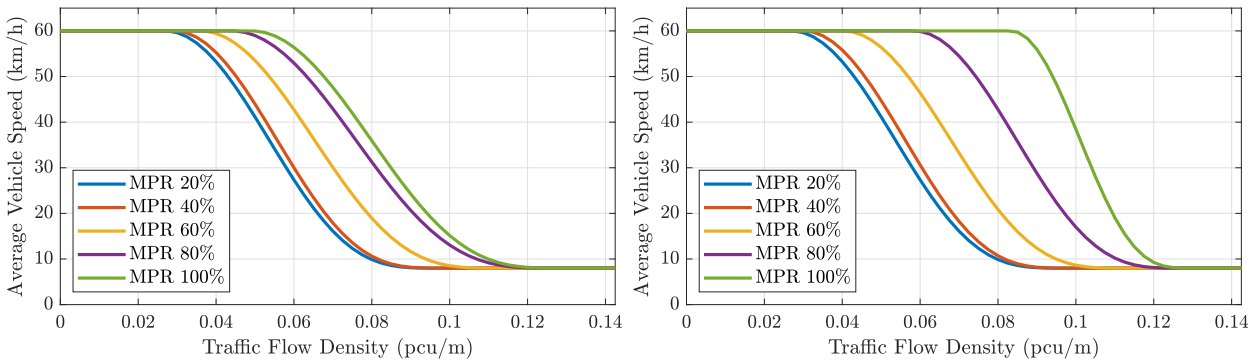

(a) No CAV coordination in road.

(b) With CAV coordination in road.

Fig. 2: Influence of CAV coordination on traffic flow performance.

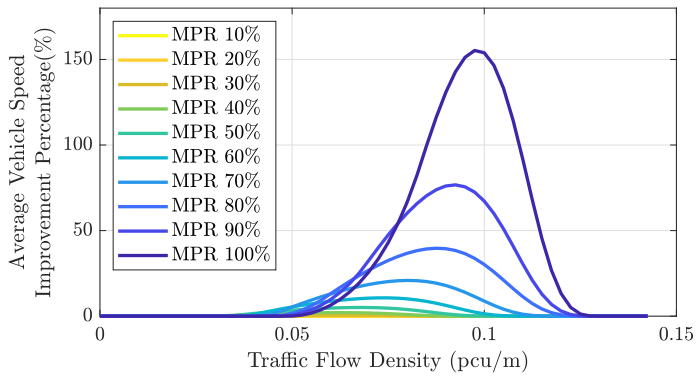

Fig. 3: Improvement percentage of road coordination.

global routing, a constraint on minimum CAV route selection ratio β_0 is imposed. Therefore,

$$\beta_{u,d,o}^{\mathrm{CAV,ctrl}}(k) > \beta_{u,d,o}(k) \cdot \beta_0. \tag{54}$$

After all CAV route selection rates are determined, a route planing algorithm can be adopted to generate the route of each CAV. The actual arriving number of vehicles is

$$\begin{aligned} m_{u,d,o}^{\mathrm{arr,CAV}}(k) &= \beta_{u,d,o}^{\mathrm{CAV,ctrl}}(k) \cdot m_{u,d}^{\mathrm{arr,CAV}}(k), \\ m_{u,d,o}^{\mathrm{arr,HDV}}(k) &= \beta_{u,d,o}(k) \cdot \left(m_{u,d}^{\mathrm{arr}}(k) - m_{u,d}^{\mathrm{arr,CAV}}(k) \right), \\ m_{u,d,o}^{\mathrm{arr}}(k) &= m_{u,d,o}^{\mathrm{arr,HDV}}(k) + m_{u,d,o}^{\mathrm{arr,CAV}}(k), \end{aligned} \tag{55}$$

where $m_{u,d,o}^{\mathrm{arr,HDV}}(k)$ is the HDV number on road (u, d) heading to intersection o at time k.

IV. Simulation Results

A. Road coordination results

It can be inferred from Section III-A that road coordination is the most effective optimization method in vehicle coordination. Numerical simulations are conducted to show the improvements. The headway time of HDV and CAV according to [37] is defined in Table. I.

As shown in Fig. 2, passenger car unit (PCU) is used to measure the traffic flow density. The relationship of average vehicle speed and traffic flow density without and with road coordination is shown in Figs. 2a, and 2b, respectively. In both cases, the average vehicle speed drops as traffic flow density increases. In addition, the increasing MPR leads to higher vehicle speed for the same traffic flow density due to the CAV's outstanding car-following distance. When coordination between the CAVs is activated, the performance can be further enhanced.

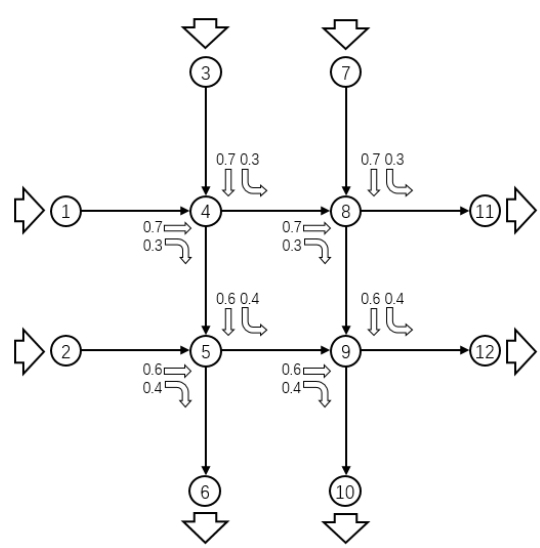

Fig. 4: Simulated Road Network.

Fig. 3 shows the improvement percentage of road coordination. We conclude that the vehicle speed improvement

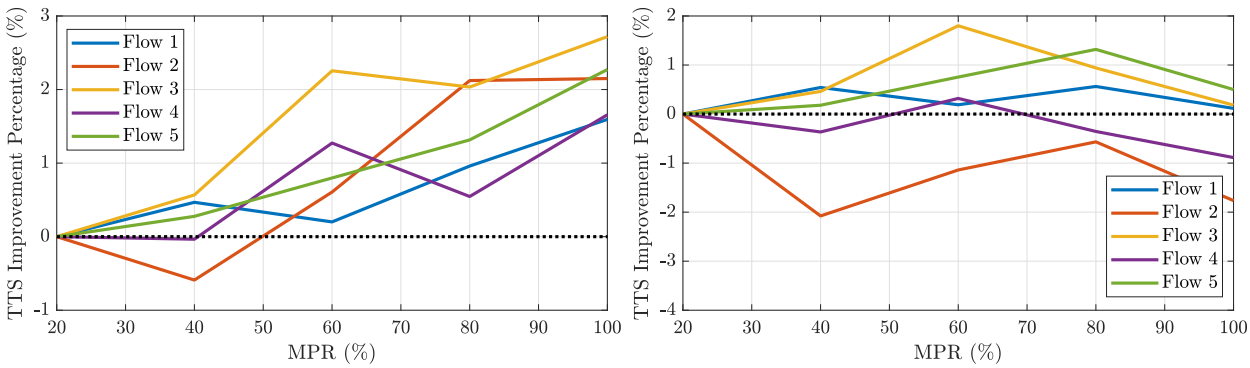

(a) With CAV coordination in network.

(b) No CAV coordination in network.

Fig. 5: Comparison of network coordination and traffic light control results.

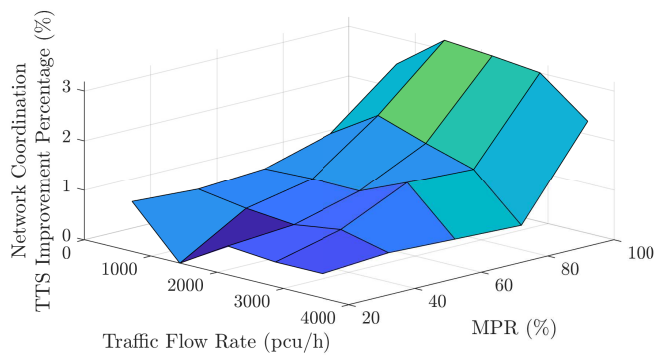

Fig. 6: Simulation results of total time spent in the road network.

function is a uni-modal function to traffic flow density. The maximum optimization percentage occurs in $0.1\,\mathrm{pcu/m}$, and the optimization is obvious when MPR is larger than 20%.

B. Traffic network simulation scenario

For analyzing the performance of the proposed coordination control method with the proposed traffic model, simulation experiments were conducted in MATLAB. Fig. 4 shows the road network used for simulation. For each road, the length is $200\,\mathrm{m}$, the number of lanes is four, and the speed limit is $60\mathrm{km/h}$. The maximum flow rate of a straight lane, a turning lane, and a road from the source road is $2\mathrm{veh/s}$, $1\mathrm{veh/s}$, and $3\mathrm{veh/s}$, respectively. This road network is designed to reproduce the rush-hour urban unbalanced traffic condition, where most traffic travels through the road network in one direction (from northwest to southeast in this road network). In addition, some roads experience a heavier traffic burden compared to adjacent roads. In this experiment, parameters of traffic input are traffic flow rate and CAV penetration rate, as listed in Table II, where the flow rate and penetration rate of roads (2,5) and (7,8) are 60% of those of roads (1,4) and (3,4). Tests were conducted for different combinations of these two parameters of roads (1,4) and (3,4). The sampling period T_s is 1s, the control horizon T_c is 100s, and the traffic input is constant over the control horizon. Route selection ratios for HDVs are shown in Fig. 4, and the minimum CAV route selection ratio $\beta_{\min}$ is 20%. The traffic light control method using a genetic algorithm was simulated under similar conditions for comparison with the proposed coordination control method for optimization.

C. Evaluation index

The simulated primary evaluation index is the total time spent (TTS) by vehicles in the road network, which is defined as

$$TTS = T_\mathrm{s} \sum_{i=1}^{k} \sum_{j=1}^{i} \left(\sum_{e \in \mathbb{E}_\mathrm{src}} m_e^{\mathrm{arr}}(j) - \sum_{e \in \mathbb{E}_\mathrm{snk}} m_e^{\mathrm{dep}}(j) \right) \quad (56)$$

where T_s is the control horizon, $\mathbb{E}_\mathrm{src}$ and $\mathbb{E}_\mathrm{snk}$ are node pair sets of all roads starting from the source node and ending at the sink node, respectively. In this case, vehicles waiting on roads from the source node are considered, implying that the TTS calculation is feasible for different traffic conditions.

D. Network coordination results

Simulation results of network coordination are shown in Fig. 5. Under the proposed coordination control, TTS has a negative relationship with MPR, which validates the benefit of the proposed method and the advantage of a high CAV penetration rate. Under traffic light control, there is a weak relationship between TTS and CAV penetration rate, indicating that traffic light control has a poor capability of utilizing individual CAV in mixed traffic.

The improvement in TTS under the coordination control compared to that under the traffic light control is shown in Fig. 6. The improvement is positive except for the condition of low traffic burden and low CAV penetration rate, which validates the advantage of the coordination control over the traffic light control. The improvement is positively correlated with CAV penetration rate, indicating that the coordination control can effectively utilize CAVs to improve traffic efficiency. In addition, coordination control has better performance when the input traffic flow is medium for a fixed penetration rate.

V. Conclusion

This paper proposes a novel macroscopic traffic model for mixed traffic networks while solving the non-conservation problem in existing modeling methods. Because CAVs are explicitly considered in modeling, their ability to improve traffic mobility is also investigated. Typical coordination algorithms are further tested on the proposed model. Specifically, road, intersection, and network coordination algorithms are verified. The impact of traffic flow rate and MPR on algorithm performance is also discussed. The traffic simulation results show that the proposed network-based coordination algorithm outperforms the traditional traffic light method in various MPRs and traffic flow rates.

A possible research prospect in this area is to consider the fuel economy in the optimization, i.e., to study multi-objective optimization. Moreover, because precise modeling of traffic networks is a complicated task, the proposed model can also be extended to learning-based or reinforcement learning methods to improve the performance.

VI. Declarations

A. Availability of data and materials

Not applicable

B. Competing interests

The authors declare no competing financial interests.

C. Funding

This work was supported by the National Natural Science Foundation of China under Grant 52072212, China Intelligent and Connected Vehicles (Beijing) Research Institute Co., Ltd., Dongfeng Automobile Co., Ltd and Key-Area Research and Development Program of Guangdong Province under Grant 2019B090912001.

D. Authors' contributions

Qing Xu and Chaoyi Chen were in charge of the whole manuscript. Qing Xu, Chaoyi Chen, and Xueyang Chang performed the review and wrote the manuscript. Xueyang Chang and Dongpu Cao proposed the main idea of the article. Qing Xu,Chaoyi Chen and Xueyang Chang provided the mathematical analysis. Qing Xu, Mengchi Cai, Jiawei Wang conducted the simulations. Dongpu Cao, Keqiang Li and Jianqiang Wang helped to check and revise the manuscript. All authors read and approved the final manuscript.

E. Acknowledgments

Not applicable.

References

[1] F. van Wageningen-Kessels, H. Van Lint, K. Vuik, and S. Hoogendoorn, "Genealogy of traffic flow models," *EURO Journal on Transportation and Logistics*, vol. 4, no. 4, pp. 445–473, 2015.

[2] A. Messner and M. Papageorgiou, "Metanet: A macroscopic simulation program for motorway networks," *Traffic engineering & control*, vol. 31, no. 8-9, pp. 466–470, 1990.

[3] A. Kotsialos, M. Papageorgiou, C. Diakaki, Y. Pavlis, and F. Middelham, "Traffic flow modeling of large-scale motorway networks using the macroscopic modeling tool metanet," *IEEE Transactions on intelligent transportation systems*, vol. 3, no. 4, pp. 282–292, 2002.

[4] X.-Y. Lu, T. Z. Qiu, R. Horowitz, A. Chow, and S. Shladover, "Metanet model improvement for traffic control," in *2011 14th International IEEE Conference on Intelligent Transportation Systems (ITSC)*. IEEE, 2011, pp. 2148–2153.

[5] M. J. Lighthill and G. B. Whitham, "On kinematic waves ii. a theory of traffic flow on long crowded roads," *Proceedings of the Royal Society of London. Series A. Mathematical and Physical Sciences*, vol. 229, no. 1178, pp. 317–345, 1955.

[6] P. I. Richards, "Shock waves on the highway," *Operations research*, vol. 4, no. 1, pp. 42–51, 1956.

[7] M. Herty and A. Klar, "Modeling, simulation, and optimization of traffic flow networks," *SIAM Journal on Scientific Computing*, vol. 25, no. 3, pp. 1066–1087, 2003.

[8] J.-P. Lebacque, "Intersection modeling, application to macroscopic network traffic flow models and traffic management," in *Traffic and Granular Flow'03*. Springer, 2005, pp. 261–278.

[9] D. Ngoduy, "Multiclass first-order modelling of traffic networks using discontinuous flow-density relationships," *Transportmetrica*, vol. 6, no. 2, pp. 121–141, 2010.

[10] H. J. Ruskin and R. Wang, "Modeling traffic flow at an urban unsignalized intersection," in *International Conference on Computational Science*. Springer, 2002, pp. 381–390.

[11] M. E. Foulaadvand and S. Belbasi, "Vehicular traffic flow at a non-signalized intersection," *Journal of Physics A: Mathematical and Theoretical*, vol. 40, no. 29, p. 8289, 2007.

[12] C. Diakaki, "Integrated control of traffic flow in corridor networks," Ph.D. dissertation, Department of Production Engineering and Management, Technical University of ..., 1999.

[13] A. Barisone, D. Giglio, R. Minciardi, and R. Poggi, "A macroscopic traffic model for real-time optimization of signalized urban areas," in *Proceedings of the 41st IEEE Conference on Decision and Control, 2002.*, vol. 1. IEEE, 2002, pp. 900–903.

[14] M. Dotoli and M. P. Fanti, "An urban traffic network model via coloured timed petri nets," *Control Engineering Practice*, vol. 14, no. 10, pp. 1213–1229, 2006.

[15] J. Wu, F. Yan, and J. Liu, "Effectiveness proving and control of platoon-based vehicular cyber-physical systems," *IEEE Access*, vol. 6, pp. 21 140–21 151, 2018.

[16] M. Keyvan-Ekbatani, A. Kouvelas, I. Papamichail, and M. Papageorgiou, "Exploiting the fundamental diagram of urban networks for feedback-based gating," *Transportation Research Part B: Methodological*, vol. 46, no. 10, pp. 1393–1403, 2012.

[17] A. Csikós, T. Tettamanti, and I. Varga, "Nonlinear gating control for urban road traffic network using the network fundamental diagram," *Journal of Advanced Transportation*, vol. 49, no. 5, pp. 597–615, 2015.

[18] S. Lin, B. De Schutter, Y. Xi, and J. Hellendoorn, "A simplified macroscopic urban traffic network model for model-based predictive control," *IFAC Proceedings Volumes*, vol. 42, no. 15, pp. 286–291, 2009.

[19] A. Jamshidnejad, S. Lin, Y. Xi, and B. De Schutter, "Corrections to "integrated urban traffic control for the reduction of travel delays and emissions"[dec 13 1609-1619]," *IEEE Transactions on Intelligent Transportation Systems*, vol. 20, no. 5, pp. 1978–1983, 2018.

[20] L. J. C. W. L. Bichun, "Activity-based control architecture for intelligent vehicle navigation," *Chinese Journal of Mechanical Engineering*, vol. 7, 2007.

[21] M. Amoozadeh, H. Deng, C.-N. Chuah, H. M. Zhang, and D. Ghosal, "Platoon management with cooperative adaptive cruise control enabled by vanet," *Vehicular communications*, vol. 2, no. 2, pp. 110–123, 2015.

[22] C. Wang, S. Gong, A. Zhou, T. Li, and S. Peeta, "Cooperative adaptive cruise control for connected autonomous vehicles by factoring communication-related constraints," *Transportation Research Part C: Emerging Technologies*, 2019.

[23] X.-Y. Lu, J. Wang, S. E. Li, and Y. Zheng, "Multiple-vehicle longitudinal collision mitigation by coordinated brake control," *Mathematical Problems in Engineering*, vol. 2014, 2014.

[24] R. Scarinci and B. Heydecker, "Control concepts for facilitating motorway on-ramp merging using intelligent vehicles," *Transport reviews*, vol. 34, no. 6, pp. 775–797, 2014.

[25] B. Xu, X. J. Ban, Y. Bian, W. Li, J. Wang, S. E. Li, and K. Li, "Cooperative method of traffic signal optimization and speed control of connected vehicles at isolated intersections," *IEEE Transactions on Intelligent Transportation Systems*, vol. 20, no. 4, pp. 1390–1403, 2018.

[26] C. Chen, Q. Xu, M. Cai, J. Wang, J. Wang, B. Xu, and K. Li, "Conflict-free cooperation method for connected and automated vehicles at unsignalized intersections: Graph-based modeling and optimality analysis," *arXiv preprint arXiv:2107.07179*, 2021.

[27] Y. Luo, Y. Xiang, K. Cao, and K. Li, "A dynamic automated lane change maneuver based on vehicle-to-vehicle communication," *Transportation Research Part C: Emerging Technologies*, vol. 62, pp. 87–102, 2016.

[28] E. S. Kazerooni and J. Ploeg, "Interaction protocols for cooperative merging and lane reduction scenarios," in *2015 IEEE 18th International Conference on Intelligent Transportation Systems*. IEEE, 2015, pp. 1964–1970.

[29] M. Cai, C. Chen, J. Wang, Q. Xu, K. Li, J. Wang, and X. Wu, "Formation control with lane preference for connected and automated vehicles in multi-lane scenarios," *arXiv preprint arXiv:2106.11763*, 2021.

[30] Y. Chen, J. Han, and H. Wu, "Quadratic programming-based approach for autonomous vehicle path planning in space," *Chinese Journal of Mechanical Engineering*, vol. 25, no. 4, pp. 665–673, 2012.

[31] F. Lin, Y. Zhang, Y. Zhao, G. Yin, H. Zhang, and K. Wang, "Trajectory tracking of autonomous vehicle with the fusion of dyc and longitudinal–lateral control," *Chinese Journal of Mechanical Engineering*, vol. 32, no. 1, pp. 1–16, 2019.

[32] J. Wang, Y. Zheng, C. Chen, Q. Xu, and K. Li, "Leading cruise control in mixed traffic flow: System modeling, controllability, and string stability," *IEEE Transactions on Intelligent Transportation Systems*, 2021.

[33] C. Chen, J. Wang, Q. Xu, J. Wang, and K. Li, "Mixed platoon control of automated and human-driven vehicles at a signalized intersection: dynamical analysis and optimal control," *Transportation Research Part C: Emerging Technologies*, vol. 127, p. 103138, 2021.

[34] A. Bose and P. Ioannou, "Mixed manual/semi-automated traffic: a macroscopic analysis," *Transportation Research Part C: Emerging Technologies*, vol. 11, no. 6, pp. 439–462, 2003.

[35] T. Tettamanti, I. Varga, and Z. Szalay, "Impacts of autonomous cars from a traffic engineering perspective," *Periodica Polytechnica Transportation Engineering*, vol. 44, no. 4, pp. 244–250, 2016.

[36] S. Calvert, W. Schakel, and J. Van Lint, "Will automated vehicles negatively impact traffic flow?" *Journal of Advanced Transportation*, vol. 2017, 2017.

[37] B. Friedrich, "The effect of autonomous vehicles on traffic," in *Autonomous Driving*. Springer, 2016, pp. 317–334.

[38] W.-X. Zhu and H. Zhang, "Analysis of mixed traffic flow with human-driving and autonomous cars based on car-following model," *Physica A: Statistical Mechanics and its Applications*, vol. 496, pp. 274–285, 2018.

[39] M. Dotoli, M. P. Fanti, and C. Meloni, "A signal timing plan formulation for urban traffic control," *Control engineering practice*, vol. 14, no. 11, pp. 1297–1311, 2006.

[40] K. Aboudolas, M. Papageorgiou, and E. Kosmatopoulos, "Store-and-forward based methods for the signal control problem in large-scale congested urban road networks," *Transportation Research Part C: Emerging Technologies*, vol. 17, no. 2, pp. 163–174, 2009.

[41] S. Lin, B. De Schutter, Y. Xi, and H. Hellendoorn, "Efficient network-wide model-based predictive control for urban traffic networks," *Transportation Research Part C: Emerging Technologies*, vol. 24, pp. 122–140, 2012.

[42] Z. Zhou, S. Lin, Y. Xi, D. Li, and J. Zhang, "A hierarchical urban network control with integration of demand balance and traffic signal coordination," *IFAC-PapersOnLine*, vol. 49, no. 3, pp. 31–36, 2016.

[43] S. Lin, Q.-J. Kong, and Q. Huang, "A model-based demand-balancing control for dynamically divided multiple urban subnetworks," *Journal of Advanced Transportation*, vol. 50, no. 6, pp. 1046–1060, 2016.

[44] Z. Zhou, B. De Schutter, S. Lin, and Y. Xi, "Two-level hierarchical model-based predictive control for large-scale urban traffic networks," *IEEE Transactions on Control Systems Technology*, vol. 25, no. 2, pp. 496–508, 2016.

[45] D. E. Kaufman, J. Nonis, and R. L. Smith, "A mixed integer linear programming model for dynamic route guidance," *Transportation Research Part B: Methodological*, vol. 32, no. 6, pp. 431–440, 1998.

[46] X. Yang and W. W. Recker, "Modeling dynamic vehicle navigation in a self-organizing, peer-to-peer, distributed traffic information system," *Journal of intelligent transportation Systems*, vol. 10, no. 4, pp. 185–204, 2006.

[47] Z. Cao, S. Jiang, J. Zhang, and H. Guo, "A unified framework for vehicle rerouting and traffic light control to reduce traffic congestion," *IEEE transactions on intelligent transportation systems*, vol. 18, no. 7, pp. 1958–1973, 2016.

[48] S. Wang, S. Djahel, and J. McManis, "A multi-agent based vehicles re-routing system for unexpected traffic congestion avoidance," in *17th International IEEE Conference on Intelligent Transportation Systems (ITSC)*. IEEE, 2014, pp. 2541–2548.

[49] A. M. de Souza, R. S. Yokoyama, L. C. Botega, R. I. Meneguette, and L. A. Villas, "Scorpion: A solution using cooperative rerouting to prevent congestion and improve traffic condition," in *2015 IEEE international conference on computer and information technology; ubiquitous computing and communications; dependable, autonomic and secure computing; pervasive intelligence and computing*. IEEE, 2015, pp. 497–503.

[50] N. Mehr and R. Horowitz, "How will the presence of autonomous vehicles affect the equilibrium state of traffic networks?" *IEEE Transactions on Control of Network Systems*, vol. 7, no. 1, pp. 96–105, 2019.

[51] A. Houshmand, S. Wollenstein-Betech, and C. G. Cassandras, "The penetration rate effect of connected and automated vehicles in mixed traffic routing," in *2019 IEEE Intelligent Transportation Systems Conference (ITSC)*. IEEE, 2019, pp. 1755–1760.

[52] F. Yan, F. Tian, and Z. Shi, "An improved traffic network model for model-based predictive control," in *Proceedings of the 33rd Chinese Control Conference*. IEEE, 2014, pp. 3405–3410.

[53] M. V. Ala, H. Yang, and H. Rakha, "Modeling evaluation of eco–cooperative adaptive cruise control in vicinity of signalized intersections," *Transportation Research Record*, vol. 2559, no. 1, pp. 108–119, 2016.

Qing Xu received his B.S. and M.S. degrees in automotive engineering from Beihang University, Beijing, China, in 2006 and 2008, respectively, and the Ph.D. degree in automotive engineering from Beihang University in 2014.

During his Ph.D. research, he worked as a Visiting Scholar with the Department of Mechanical Science and Engineering, University of Illinois at Urbana–Champaign. From 2014 to 2016, he had his postdoctoral research at Tsinghua University. He is currently working as an Assistant Research Professor with the School of Vehicle and Mobility, Tsinghua University. His main research interests include decision and control of intelligent vehicles.

Chaoyi Chen (Graduate Student Member, IEEE) received the B.E. degree from Tsinghua University, Beijing, China, in 2016, and the M.S. from Tsinghua University, Beijing, China, and RWTH Aachen University, Aachen, Germany in 2019. He is currently a Ph.D. student in mechanical engineering with the School of Vehicle and Mobility, Tsinghua University. He was a recipient of the Scholarship of Strategic Partnership RWTH Aachen University and Tsinghua University. His research interests include vehicular networks, control theory, and cooperative control.

Xueyang Chang received his B.S. and Ph.D. degree in mechanical engineering from Tsinghua University, Beijing, China, in 2015 and 2021, respectively. He is currently a cloud control technical expert with the Tsingcloud Co., Lmt. His main research interests include decision and control of intelligent vehicles and cloud control systems.

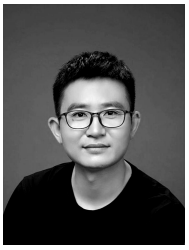

Dongpu Cao received the Ph.D. degree from Concordia University, Canada, in 2008. He is the Canada Research Chair in Driver Cognition and Automated Driving, and an Associate Professor at University of Waterloo. His current research focuses on driver cognition, automated driving and cognitive autonomous driving. He has contributed more than 200 papers and 3 books. He received the SAE Arch T. Colwell Merit Award in 2012, IEEE VTS 2020 Best Vehicular Electronics Paper Award, 2021 IEEE ITSS Outstanding Application Award, and 7 Best Paper Awards from international conferences. Prof. Cao has served as Deputy Editor-in-Chief for IET INTELLIGENT TRANSPORT SYSTEMS JOURNAL, and an Associate Editor for IEEE TRANSACTIONS ON VEHICULAR TECHNOLOGY, IEEE TRANSACTIONS ON INTELLIGENT TRANSPORTATION SYSTEMS and other journals. Prof. Cao is an IEEE VTS Distinguished Lecturer.

Mengchi Cai (Graduate Student Member, IEEE) received the B.E. degree from Tsinghua University, Beijing, China, in 2018. He is currently a Ph.D. candidate in mechanical engineering with the School of Vehicle and Mobility, Tsinghua University. His research interests include connected and automated vehicles, multi-vehicle formation control, and unsignalized intersection cooperation.

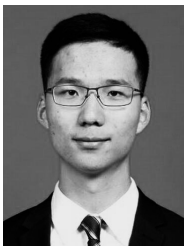

Jiawei Wang (Graduate Student Member, IEEE) received the B.E. degree from Tsinghua University, Beijing, China, in 2018. He is currently a Ph.D. student in mechanical engineering with the School of Vehicle and Mobility, Tsinghua University. His research interests include connected automated vehicles, distributed control and optimization, and data-driven control. He was a recipient of the National Scholarship in Tsinghua University. He received the Best Paper Award at the 18th COTA International Conference of Transportation Professionals.

Keqiang Li received the B.Tech. degree from Tsinghua University of China, Beijing, China, in 1985, and the M.S. and Ph.D. degrees in mechanical engineering from the Chongqing University of China, Chongqing, China, in 1988 and 1995, respectively.

He is currently a Professor with the School of Vehicle and Mobility, Tsinghua University. His main research areas include automotive control system, driver assistance system, and networked dynamics and control, and is leading the national key project on CAVs (Intelligent and Connected Vehicles) in China. Dr. Li has authored more than 200 papers and is a co-inventor of over 80 patents in China and Japan.

Dr. Li has served as a Fellow Member of Society of Automotive Engineers of China, editorial boards of the *International Journal of Vehicle Autonomous Systems*, Chairperson of Expert Committee of the China Industrial Technology Innovation Strategic Alliance for CAVs (CACAV), and CTO of China CAV Research Institute Company Ltd. (CCAV). He has been a recipient of Changjiang Scholar Program Professor, National Award for Technological Invention in China, etc.

Jianqiang Wang received the B. Tech. and M.S. degrees from Jilin University of Technology, Changchun, China, in 1994 and 1997, respectively, and the Ph.D. degree from Jilin University, Changchun, in 2002. He is currently a Professor with the School of Vehicle and Mobility, Tsinghua University, Beijing, China.

He has authored over 150 papers and is a co-inventor of 99 patent applications. He was involved in over 10 sponsored projects. His active research interests include intelligent vehicles, driving assistance systems, and driver behavior. He was a recipient of the Best Paper Award in the 2014 IEEE Intelligent Vehicle Symposium, the Best Paper Award in the 14th ITS Asia Pacific Forum, the Best Paper Award in the 2017 IEEE Intelligent Vehicle Symposium, the Changjiang Scholar Program Professor in 2017, the Distinguished Young Scientists of NSF China in 2016, and the New Century Excellent Talents in 2008.